

## Site-to-bedrock over 1D transfer function ratio: An indicator of the proportion of edge-generated surface waves?

Cécile Cornou<sup>1</sup> and Pierre-Yves Bard<sup>1,2</sup>

Laboratoire de Géophysique Interne et Tectonophysique, Université Joseph Fourier, Grenoble, France

Received 11 November 2002; revised 5 February 2003; accepted 4 March 2003; published 2 May 2003.

[1] We study multi-dimensional site effects in the small-size deep sediment filled basin of Grenoble (French Alps). A very dense array composed of 3-component seismometers over a 1 km aperture is used to investigate propagation parameters of waves propagating across the array. We present results for 6 teleseismic events for which we had a reference rock site. For the frequency range 0.1 to 1 Hz, records are clearly dominated by edge-generated surface waves. Quantification of energy carried by each identified wave train allows interpreting the difference between site-to-bedrock and 1D transfer function estimates in terms of laterally propagating basin-edge induced waves only above the fundamental resonance frequency of the basin. A simple ratio between site-to-bedrock and 1D transfer function curves should thus provide an estimation of the relative contribution of 1D and 2D/3D effects in ground motion on the condition that all the time signal length is taken into account. **INDEX TERMS:** 7212 Seismology: Earthquake ground motions and engineering; 7223 Seismology: Seismic hazard assessment and prediction; 7294 Seismology: Instruments and techniques. **Citation:** Cornou, C., and P.-Y. Bard, Site-to-bedrock over 1D transfer function ratio: An indicator of the proportion of edge-generated surface waves?, *Geophys. Res. Lett.*, 30(9), 1453, doi:10.1029/2002GL016593, 2003.

### 1. Introduction

[2] It has long been recognized that near-surface geological conditions play a significant role in modifying earthquake ground motion. A common explanation for the amplification of motion is the body wave trapping effects due to the impedance contrast between horizontally layered sediments and underlying bedrock. When the local soil profile is known, the site amplification is routinely evaluated in the frequency domain by computing the 1D transfer function. In case of a 2D or 3D structure however, this trapping also affects the surface waves, which develop on those heterogeneities and are subsequently trapped within the structure. By increasing amplification, duration and spatial variability of ground motion, the locally generated surface waves become very important for the local damage distribution [Kawase, 1996]. Despite this, they are not accounted for in site effects studies that most often focus or refer to effects of 1D structure only. The main reason for this is much more the difficulty in grasping edge-generated

surface waves in seismograms than physics in play as it has been shown by the large theoretical and numerical literature about site effects modeling [e.g., Graves, 1996]. For basins of small or medium size (with widths and thickness smaller than a few hundred meters and 10 km, respectively) direct S-waves and basin-edge induced waves are mixed and, in addition, 1D and 2D/3D effects contribute to the same frequency band. Their separation in the frequency domain is therefore difficult [Chavez-Garcia and Faccioli, 2000]. So far, multi-dimensional site effects have been most often brought up from the failure of 1D modeling to predict actual amplification (derived from experimental site-to-bedrock ratio [Borcherdt, 1970]), or duration. This failure is spectacular in small-size and deep sedimentary alpine valleys [Lebrun et al., 2001; Faccioli et al., 2002]. The Grenoble basin (French Alps) is such an example (Figure 1): whereas the site-to-bedrock spectral ratio shows a flat amplification of huge magnitude 0.25 Hz [Lebrun et al., 2001] to 5 Hz, this effect cannot be seen on other curves derived either from 1D modeling either from H over V ratio on microtremors. In a previous study (C. Cornou et al., Contribution of dense array analysis to the identification and quantification of basin-edge induced waves. part II: Application to Grenoble basin (French Alps), submitted to *Bulletin of the Seismological Society of America*, 2002b, hereinafter referred to as Cornou et al., submitted manuscript, 2002b), a very dense array of seismometers was installed within the city of Grenoble. Locally generated surface waves could be directly identified and characterized using an array processing technique. Energy carried by each identified wave train could be quantified. Using such energy estimates, this paper provides new insights in understanding 2D/3D site effects through interpretation of the difference between site-to-bedrock and theoretical 1D estimates.

### 2. Characterizing Edge-Generated Surface Waves at Low Frequencies (<1 Hz)

#### 2.1. Grenoble Basin, Data and Method

[3] The Y-shaped sedimentary fill of the Grenoble basin consists of late quaternary post-glacial deposits overlaying a marly Jurassic limestone bedrock. Both geometry and mechanical properties of the basin were inferred from gravimetric [Vallon, 1999], active reflection and refraction seismic [Dietrich et al., 2001] and microtremor recordings studies [Lebrun et al., 2001], which have been calibrated by a deep borehole drilled in the NE branch of the valley. The sediment thickness reaches 900 m in the central part of the basin, which is at most 5 km wide.

[4] An array consisting of 29 three-component seismic sensors (Figure 2) was installed in the eastern part of the

<sup>1</sup>Now at Institute of Geophysics, Eidgenössische Technische Hochschule, Zürich, Switzerland.

<sup>2</sup>Also at Laboratoire Central des Ponts-et-Chaussées, Paris, France.

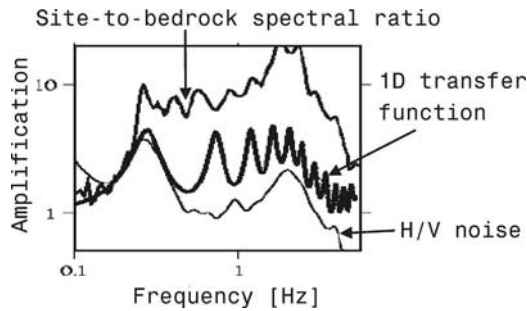


**Figure 1.** Example of site-to-bedrock obtained in Grenoble city for a 2.5 Ml seismic event occurred 15 km far from the basin, 1D transfer function and H over V ratio on microtremors.

city. The array was equipped with short-period sensors (16 MarkProducts L22, flat response from 2 to 50 Hz) and wider-band sensors (13 Lennartz Le3D/Guralp CMG40 with a flat response from 0.2/0.05 to 50 Hz). The experiment lasted 4 months during spring 1999 and recorded teleseismic, regional and local events (weak motions). As we are interested in this paper in comparing 1D and site-to-bedrock estimates, we only consider teleseismic events for which we had a reference rock site (SSB broadband station of the Geoscope permanent network). Six teleseismic events are thus selected based on their satisfactory signal-to-noise ratio. They were recorded at least on 8 wide-band sensors. The array analysis allows to identifying frequency, back-azimuth and apparent velocities of wave fronts crossing an array. For the whole signal time length, we first track the time-frequency windows for which waveforms are the most coherent across the whole array. The *Multiple Signal Characterization* (MUSIC) [Schmidt, 1981] technique is then applied on these domains. Within an additive spatial smoothing procedure (C. Cornou et al., Contribution of dense array analysis to the identification and quantification of basin-edge induced waves. part I: Methodology, submitted to *Bulletin of the Seismological Society of America*, 2002a, hereinafter referred to as Cornou et al., submitted manuscript, 2002a), MUSIC is indeed well adapted to handle with the large complexity of wave propagation including multiple and/or correlated phases that are strongly expected in such a small 3D structure.

[5] The analysis was performed between 0.1 and 1 Hz separately on each component. We only kept time occurrence and propagation parameters of those waves similarly identified on both horizontal components within a time, back-azimuth and frequency deviation of 5 s,  $10^\circ$  and 0.05 Hz, respectively. Next, the average analytical 3-component covariance matrix is used to evaluate energy carried by each identified wave train [Vidale, 1986]. The energy estimation is corrected to possibly account for effects of other wave trains propagating at the same time across the array (Cornou et al., submitted manuscript, 2002a).

## 2.2. Origin and Nature of Diffracted Wave Field

[6] We assume that direct waves are waves coming from the source area within a back-azimuth deviation of  $\pm 30^\circ$  from the theoretical back-azimuth to account for some deviation of the incident wave field by regional heterogeneities outside the basin [Cotte et al., 2000]. The diffracted

waves correspond to all other waves. It means that we may only overestimate the source term, since there may exist diffracted waves in the epicentral azimuth. Despite a significant event-to-event source location variation, diffracted wave trains exhibit two main stable directions of propagation coming clearly from the two closest basin edges, underlying thus the importance of 3D structure in shaping wave field (Figure 3a). Figure 3b shows that apparent velocities are low at high frequencies and larger for low frequencies. In addition, phase velocities lie between the theoretical dispersion curves of the first modes of Love and Rayleigh waves derived from the borehole velocity model. Spatial origin and phase velocities variation with frequency strongly argue that identified diffracted waves are basin-edge induced surface waves. Comparing cumulative energy over time of filtered signals between 0.1 and 1 Hz and identified wave trains, C. Cornou et al. (submitted manuscript, 2002b) has shown that almost 40% of the total energy of seismogram was explained using array technique, the remaining 60% corresponding to incoherent waveforms traveling across the array that could not be analyzed with array technique. The prevalence of energy scattered from lateral heterogeneity was also outlined: diffracted waves carry four times more energy than direct waves.

## 2.3. Comparison Between Standard Spectral Ratio and 1D Transfer Function

[7] Geometrical site effects can be seen as the combination of 1D and 2D/3D site effects acting together. The horizontal spectrum on soft deposits can be thus decomposed as follows:  $H = H^{1D} + H^{2D/3D}$  where  $H^{1D}$  and  $H^{2D/3D}$  are the horizontal spectra related to 1D and 2D/3D site effects, respectively. If we assume now that direct waves are mainly affected by the local soil-column properties (vertical reverberations of body waves, 1D effects) and that edge-generated surface waves laterally reverberating reflect thus 2D/3D effects, the previous relation may be rewritten in the following way:

$$H = H^{1D}[1 + \alpha_0] \text{ where } \alpha_0 = \frac{H^{diff,tot}}{H^{dir,tot}} \approx \sqrt{\frac{E^{diff,tot}}{E^{dir,tot}}} \quad (1)$$

where  $H^{diff,tot}$  ( $E^{diff,tot}$ ) and  $H^{dir,tot}$  ( $E^{dir,tot}$ ) are the horizontal spectra (total energy) of total diffracted and direct wave fields, respectively. Total energy can be used to evaluate  $\alpha_0$

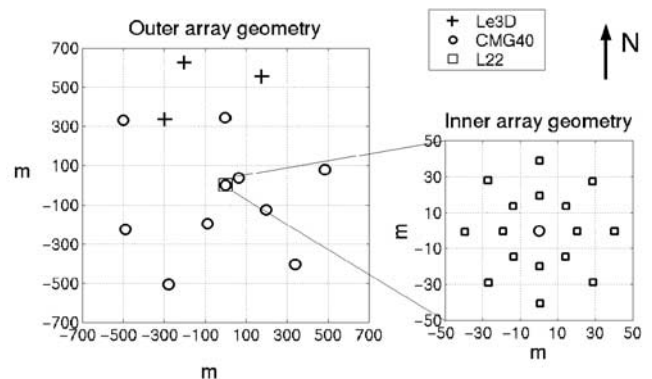


**Figure 2.** Configuration of the array.

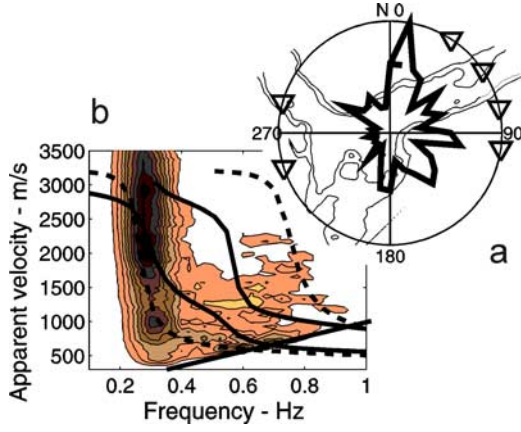


**Figure 3.** (a) Distribution of the most energetic back-azimuth diffracted wave crossing the array reported on the Grenoble basin's contour map (triangles indicate source back-azimuth). The array is located at the circle's center. Energy distribution of each event is added and averaged. (b) Distribution of apparent velocities as a function of frequency (the lines correspond to the two first modes of the Rayleigh (solid lines) and the Love (dashed lines) phase velocity dispersion curves, the straight line delimitates the velocity-frequency unreliability domain for array analysis). Distribution of velocities of each event is simply added. The color darkness is proportional to the number of identified wave trains at that velocity-frequency location.

because the vertical ground motion is much less amplified than the horizontal motion within soft deposits. Value of  $\alpha_0$  can be interpreted as the production of edge-generated surface waves in the total surface ground motion.

[8] Assuming for  $H^{1D}$  the theoretical 1D transfer function derived from the velocity model, we calculate a site-to-bedrock spectral ratio in order to compare it to the observed one. Fourier spectra amplitudes (modulus) of horizontal components of explained diffracted  $H^{diff,expl}$  and direct  $H^{dir,expl}$  waveforms are used for providing an estimate  $\alpha$  of  $\alpha_0$ . As the reference station is 100 km far from the array, we focus here on frequencies below 0.5 Hz only, to warrant similar seismic source paths.

[9] Figure 4a indicates for one event at each frequency the proportion  $\beta$  of explained energy  $E^{expl}$  compared to the total energy of seismogram  $E^{tot}$  ( $E^{expl} = \beta \cdot E^{tot}$ ) and the proportion  $\gamma$  of diffracted energy  $E^{diff,expl}$  compared to analyzed energy  $E^{expl}$  ( $E^{diff,expl} = \gamma \cdot E^{expl} = \gamma \cdot \beta \cdot E^{tot}$ ). The proportion of direct energy  $E^{dir,expl}$  compared to  $E^{expl}$  is then  $E^{dir,expl} = (1 - \gamma) \cdot \beta \cdot E^{tot}$ .

[10] When all the energy of seismogram ( $\beta = 100\%$ ) is explained with array analysis, the observed  $\alpha$  should provide an accurate estimation  $\alpha_1$  of  $\alpha_0$ :

$$E^{diff,tot} = E^{diff,expl} = \gamma \cdot E^{tot} \quad (2)$$

$$E^{dir,tot} = E^{dir,expl} = (1 - \gamma) \cdot E^{tot} \quad (3)$$

$$\alpha_1 = \left[ \frac{\gamma}{1 - \gamma} \right]^{\frac{1}{2}} \quad (4)$$

If only a portion of energy is investigated with array analysis ( $\beta < 100\%$ ) and if we assume that the non-coherent energy  $E^{not\_expl}$  that could not be analyzed with array

technique is coming only from diffracted waves ( $E^{diff,tot} = E^{diff,expl} + E^{not\_expl} = (\gamma \cdot \beta + 1 - \beta)E^{tot}$ ), an upper estimation  $\alpha_{max}$  of  $\alpha_0$  is:

$$\alpha_{max} = \alpha_1 \left[ 1 + \frac{1}{\beta \cdot \gamma} - \frac{1}{\gamma} \right]^{\frac{1}{2}} \quad (5)$$

On the contrary, if the non-coherent energy is coming only from direct waves, a lower estimation  $\alpha_{min}$  of  $\alpha_0$  is:

$$\alpha_{min} = \left[ \frac{\beta \cdot \gamma}{1 - \beta \cdot \gamma} \right]^{\frac{1}{2}} \quad (6)$$

[11] Figure 4b displays for the same event the theoretical 1D transfer function, the observed site-to-bedrock ratio (horizontal and quadratic mean horizontal components are used) and the calculated site-to-bedrock ratio (open circles). Between 0.2 and 0.3 Hz, array technique allows investigating almost all the energy of seismogram (Figure 4a, open squares) that is mostly composed of diffracted energy ( $\gamma \approx 80\%$ , Figure 4a, crosses). In agreement with relation (4), calculated site-to-bedrock ratios fit the observed curve (Figure 4b, open circles): it strongly argues for this frequency band that difference between site-to-bedrock and 1D estimates can effectively be interpreted in terms of basin-edge induced wave effects only. At higher frequencies, from 0.3 to 0.4 Hz, only 7 to 22% ( $\beta$ ) of energy could be explained. Assuming that the non-coherent energy  $E^{not\_expl}$  that could not be analyzed with array technique is coming only from diffracted waves, we use relation (5) with  $\alpha_1 = \alpha$  to boost the 0.325 and 0.375  $\alpha$  estimates. New estimated site-to-bedrock ratios (Figure 4b, crosses) fit well the actual site-to-bedrock curve. At 0.175 Hz, observed site-to-bedrock ratio overestimates the actual amplification. However,

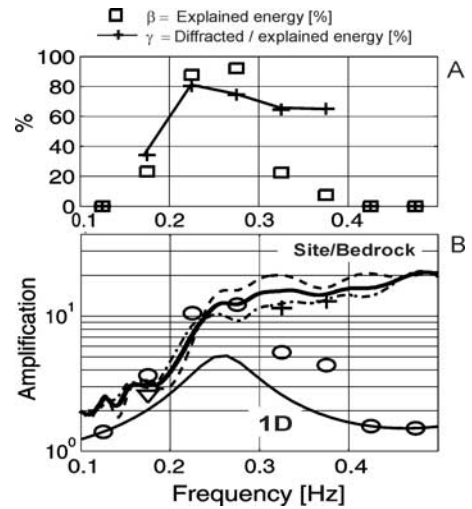


**Figure 4.** (a) Proportion of analysed energy compared to total energy of seismogram and proportion of diffracted energy compared to analysed energy as a function of frequency. The 6.3 Ms teleseismic event used occurred the 1999/05/06 at 23:00:50 UTC in Iran; (b) Site-to-bedrock spectral ratio [NS (dashed line), EW (dash-dotted line) and quadratic mean horizontal spectra (thick line)] and 1D transfer function (thin line) as a function of frequency. See text for circles, crosses and triangles explanation.

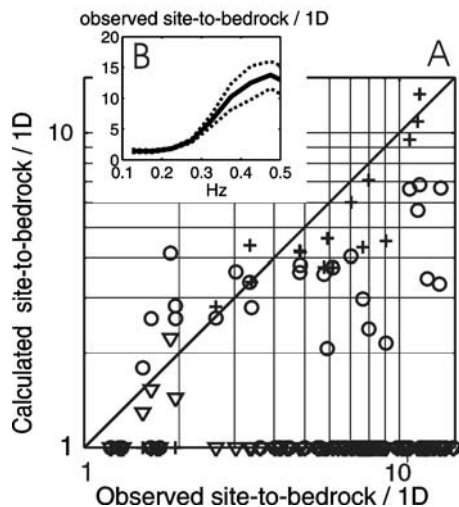


**Figure 5.** (a) Calculated site-to-bedrock over 1D estimate as a function of observed site-to-bedrock over 1D estimate for all 6 events. See text for circles, crosses and triangles explanation; (b) Using all events, the observed average site-to-bedrock ratio  $\pm$  standard deviation is also displayed as a function of frequency.

C. Cornou et al. (submitted manuscript, 2002b) have observed that incident waves with frequency content lower than the resonance frequency of the basin are not significantly influenced by the basin. According to such observations, we assume for this frequency that the non-coherent energy is coming mainly from direct waves and calculate a new 0.175 Hz  $\alpha$  estimate using relation (6). New estimated site-to-bedrock value at 0.175 Hz (Figure 4b, triangle) fit better the actual amplification.

[12] We plot for all events calculated site-to-bedrock ratio values (Figure 5a, circles). When the energy of seismogram is not completely investigated with array technique ( $\beta < 100\%$ ), we assume for frequencies above 0.25 Hz that non-coherent wave field is composed mainly of diffracted waves (considering the coherent wave field for all events, the  $\gamma$  mean value is  $85 \pm 15\%$ ) and boost previous  $\alpha$  estimates using relation (5) (Figure 5a, crosses). Such boosting is only performed when the proportion of diffracted waves  $\gamma$  is less than 90%. For frequencies below 0.25 Hz, we use relation (6) to calculate new  $\alpha$  estimates (Figure 5a, triangles). Calculated or boosted estimates most often reach the actual amplification. However, these observations argue that, above the fundamental frequency of resonance, the non-coherent wave field is mostly composed of diffracted waves and underline the major play of edge-generated surface waves in differing site-to-bedrock and 1D curves. Since site-to-bedrock spectral ratio seems to incorporate all site effects (1D and 2D/3D effects), the relative contribution of 1D and 2D/3D effects in ground motion can therefore be quantified through a ratio between site-to-bedrock and 1D

estimates. Here, 2D/3D site effects should also be responsible of a ground motion over-amplification up to 12 times the 1D amplification at 0.5 Hz (Figure 5b).

### 3. Conclusions

[13] In the Grenoble basin, array analysis on 6 teleseismic events recorded by a dense array of 3-component seismometers has shown that, between 0.1 and 0.5 Hz, the difference between site-to-rock spectral ratios and theoretical 1D transfer function seems to be produced by edge-generated surface waves only. This interpretation is not surprising since all site effects affect signal recorded on soft deposits. From earthquake engineering point of view, it means that site-to-bedrock spectral ratio incorporates 1D and all the 2D/3D site effects on the condition that the whole signal length is considered. Over-amplification of ground motion induced by 2D/3D effects compared to 1D effects only can thus be evaluated through a site-to-bedrock and 1D estimates ratio.

[14] **Acknowledgments.** We thank A. Zerva for providing the original MUSIC code. Computations were performed at the Service Commun de Calcul Intensif de l'Observatoire de Grenoble (SCCI). This work was supported by the Pôle Grenoblois des Risques Naturels and the "Programme National de Recherche sur la Prévision des Risques Naturels" de l'Institut des Sciences de l'Univers du CNRS.

### References

- Borcherdt, R. D., Effects of local geology on ground motion near San Francisco Bay, *Bull. Seismol. Soc. Am.*, *60*, 29–61, 1970.
- Chavez-Garcia, F. J., and E. Faccioli, Complex site effects and building codes: Making the lap, *J. Seimol.*, *4*, 23–40, 2000.
- Cotte, N., H. A. Pedersen, M. Campillo, V. Farra, and Y. Cansi, Off-great-circle propagation of intermediate-period surface waves observed on a dense array in the French Alps, *Geophys. J. Int.*, *142*, 825–840, 2000.
- Dietrich, M., C. Cornou, C. Bordes, P.-Y. Bard, and F. Lemeille, Geophysical exploration for site-effects assesment: Borehole measurements and Vibroseis profiling in the Isère vally near Grenoble, France, paper presented at European Geophysical Society, Nice, France, 2001.
- Faccioli, E., M. Vanini, and L. Frassiné, "Complex" site effects in earthquake strong motion, including topography, paper presented at 12th European Conference on Earthquake Engineering, Soc. Earthquake and Civ. Eng. Dyn., London, 2002.
- Graves, R. W., Simulating seismic wave propagation in 3D elastic media using staggered-grid finite differences, *Bull. Seismol. Soc. Am.*, *86*, 1091–1106, 1996.
- Kawase, H., The cause of the damage belt in Kobe: "The basin-edge effect," constructive interference of the direct S-wave with the basin-induced diffracted/Rayleigh waves, *Seismol. Res. Lett.*, *67*, 25–34, 1996.
- Lebrun, B., D. Hatzfeld, and P.-Y. Bard, A site effect study in urban area: Experimental results in Grenoble (France), *Pure Appl. Geophys.*, *158*, 2543–2557, 2001.
- Schmidt, R. O., A signal subspace approach to multiple emitter location and spectral estimation, Ph.D. diss., 201 pp., Stanford Univ., Stanford, Calif., 1981.
- Vallon, M., Estimation de l'épaisseur d'alluvions et sédiments quaternaires dans le région grenobloise par inversion des anomalies gravimétriques, IPSN/CNRS internal report, 34 pp., France, 1999.
- Vidale, J. E., Complex polarization analysis of particle motion, *Bull. Seismol. Soc. Am.*, *76*, 1393–1405, 1986.

P.-Y. Bard and C. Cornou, Laboratoire de Géophysique Interne et Tectonophysique, BP53, 38041, Grenoble Cédex 9, France. (cornou@seismo.ifg.ethz.ch)